

# Monitoring boreal forest biomass and carbon storage change by integrating airborne laser scanning, biometry and eddy covariance data



C. Hopkinson<sup>a</sup>, L. Chasmer<sup>a,\*</sup>, A.G. Barr<sup>b</sup>, N. Kljun<sup>c</sup>, T.A. Black<sup>d</sup>, J.H. McCaughey<sup>e</sup>

<sup>a</sup> Department of Geography, University of Lethbridge, Lethbridge, AB T1K 3M4, Canada

<sup>b</sup> Environment Canada, 11 Innovation Blvd, Saskatoon, SK S7N 3H5, Canada

<sup>c</sup> Department of Geography, Swansea University, Swansea, United Kingdom

<sup>d</sup> Departments of Applied Biology and Soil Science, University of British Columbia, Vancouver, BC V6T 1Z4, Canada

<sup>e</sup> Department of Geography, Queen's University, Kingston, ON K7L 3N6, Canada

## ARTICLE INFO

### Article history:

Received 7 August 2015

Received in revised form 25 March 2016

Accepted 10 April 2016

Available online 20 April 2016

### Keywords:

Net ecosystem production (NEP)

Gross primary production (GPP)

Stand growth

Change detection

Airborne laser scanning

Multi-temporal LIDAR

Jack pine chronosequence

Boreal forest

Carbon balance

Monitoring framework

## ABSTRACT

This study presents a comparison and integration of three methods commonly used to estimate the amount of forest ecosystem carbon (C) available for storage. In particular, we examine the representation of living above- and below-ground biomass change (net accumulation) using plot-level biometry and repeat airborne laser scanning (ALS) of three dimensional forest plot structure. These are compared with cumulative net CO<sub>2</sub> fluxes (net ecosystem production, NEP) from eddy covariance (EC) over a six-year period within a jack pine chronosequence of four stands (~94, 30, 14 and 3 years since establishment from 2005) located in central Saskatchewan, Canada. Combining the results of the two methods yield valuable observations on the partitioning of C within ecosystems. Subtracting total living biomass C accumulation from NEP results in a residual that represents change in soil and litter C storage. When plotted against time for the stands investigated, the curve produced is analogous to the soil C dynamics described in Covington (1981). Here, ALS biomass accumulation exceeds EC-based NEP measured in young stands, with the residual declining with age as stands regenerate and litter decomposition stabilizes. During the 50–70 year age-period, NEP and live biomass accumulation come into balance, with the soil and litter pools of stands 70–100 years post-disturbance becoming a net store of C. Biomass accumulation was greater in 2008–2011 compared to 2005–2008, with the smallest increase in the 94-year-old “old jack pine” stand and greatest in the 14-year-old “harvested jack pine 1994” stand, with values of 1.4 (± 3.2) tC ha<sup>-1</sup> and 12.0 (± 1.6) tC ha<sup>-1</sup>, respectively. The efficiency with which CO<sub>2</sub> was stored in accumulated biomass was lowest in the youngest and oldest stands, but peaked during rapid regeneration following harvest (14-year-old stand). The analysis highlights that the primary source of uncertainty in the data integration workflow is in the calculation of biomass expansion factors, and this aspect of the workflow needs to be implemented with caution to avoid large error propagations. We suggest that the adoption of integrated ALS, in situ and atmospheric flux monitoring frameworks is needed to improve spatio-temporal partitioning of C balance components at sub-decadal scale within rapidly changing forest ecosystems and for use in national carbon accounting programs.

© 2016 The Authors. Published by Elsevier Inc. This is an open access article under the CC BY-NC-ND license (<http://creativecommons.org/licenses/by-nc-nd/4.0/>).

## 1. Introduction

Net ecosystem production (NEP) represents the organic carbon (C) balance of an ecosystem through the process of sequestration and loss (Randerson, Chapin, Harden, Neff, & Harmon, 2002). Specifically, this involves the processes of photosynthesis and C import, minus losses to ecosystem respiration (Re), C export and non-biological oxidation of C (Lovett, Cole, & Pace, 2006). Given linkages between atmospheric CO<sub>2</sub> and global climate (IPCC, 2013), monitoring of continuously changing C stocks, sources and sinks, as well as associated land management or climatic feedbacks, is required for effective greenhouse gas mitigation

strategies (Canadell et al., 2007). Spatialization and partitioning of ecosystem NEP enables improved understanding of atmospheric C sequestration in biomass growth, and therefore may be linked to national C accounting programs, calibration of land surface models and diagnostic assessment of the terrestrial biosphere (Jung et al., 2011).

Reporting of C gains and losses within the terrestrial biosphere has increased in recent years as a result of these needs (Canadell et al., 2007), with national reporting guidelines set by the United Nations Framework Convention on Climate Change (UNFCCC). The need to develop and refine sophisticated C monitoring techniques are further realised through international programs like the REDD (Reducing Emissions from Deforestation and forest Degradation) and GOCF-GOLD (Global Observation of Forest and Land Cover Dynamics) programs. Examples of national agencies currently embarking on or supporting

\* Corresponding author.

E-mail address: [laura.chasmer@uleth.ca](mailto:laura.chasmer@uleth.ca) (L. Chasmer).

integrated remote sensing and in situ ecosystem-scale C monitoring and research initiatives are NEON (National Ecological Observatory Network Inc. USA, [www.neonscience.org](http://www.neonscience.org)) and TERN (Terrestrial Ecosystem Research Network, Australia, [www.tern.org.au](http://www.tern.org.au)).

Several monitoring strategies are currently in place to quantify drivers of short-term C source/sink variability and longer-term changes in ecosystem C stocks. However, approaches used to understand ecosystem C differ in terms of spatial and temporal representation, as well as the physical quantities being measured (Medvigy & Moorcroft, 2011). This has the potential to create discrepancies in greenhouse gas reporting across regions and between nations. For example, eddy covariance (EC) methods routinely provide estimates of the net ecosystem exchange (NEE) of gains and losses of CO<sub>2</sub> between soil, vegetation and atmosphere over defined time periods and spatial extents. NEE is equivalent but opposite in sign to NEP when inorganic C fluxes balance or are negligible. Gross primary production (GPP) is NEP minus R<sub>e</sub>, though is less directly observed, as ecosystem respiration (the combination of autotrophic and heterotrophic respiration) is usually modelled (Barr, Morgenstern, Black, McCaughey, & Nesic, 2006; Griffis et al., 2003). Over periods of 2 to 10 years, changes in GPP or NEP due to factors like severe drought, fire or insect/pathogen disturbances may be monitored (Barr et al., 2007; Ciais et al., 2005). However, because EC methods provide an aggregate estimate of C exchange, there are limits to how far ecosystem process, composition changes or anthropogenic vs natural influences can be partitioned or extrapolated over broad regions. Further, large uncertainties exist with regards to within-ecosystem process interaction thereby limiting the use of data-intensive ecosystem biogeochemical models (Canadell et al., 2007).

Another C assessment option uses inventory methods to monitor above and below-ground C pools within forest plots. Plots can be revisited every few years to estimate rates of biomass accumulation and partitioning associated with age, site history, and changes to management regime. Plot measurements can include direct sampling of living biomass and other C pools including roots, detritus and litterfall. These data can be used to estimate net primary production (NPP) of cumulative biomass C stored within all above and below-ground components (Law, Thornton, Irvine, Anthoni, & Van Tuyl, 2001). (Note, NEP and NPP are parallel but distinct concepts, as NPP does not account for heterotrophic respiration C losses). Above and below-ground biomass measurements can be destructive, limited in spatial extent and temporal frequency because they are labour intensive (Curtis et al., 2002; Gower et al., 1997; Lambert et al., 2005; Peichl & Arain, 2007; Zha et al., 2013), and may not fully account for spatial variability (Kristensen, Næsset, Ohlson, Bolstad, & Kolka, 2015). Despite such limitations, in situ observations of temporal change in C stocks provide a cumulative assessment of biomass C growth and loss (Barford et al., 2001), which may allow for more direct partitioning of changes in C pool quantities associated with climatic, disturbance and land management drivers.

For long-term monitoring of plot-based C pools, measurement protocols need to be consistent to ensure accurate comparisons. A challenge associated with repetitive field sampling is the possibility that by collecting measurements and samples (e.g. invasive root measurements, trampling of understory, litter traps), the observer might alter the growth trajectory of the plot or surrounding area (Cahill, Castelli, & Casper, 2001; Semboli, Beina, Closset-Kopp, Gourlet-Fleury, & Decocq, 2014). Such concerns provide justification for refining and integrating non-invasive C assessment techniques such as eddy covariance and remote sensing (He, Chen, Pan, Birdsey, & Kattge, 2012; Kristensen et al., 2015). To this end, airborne laser scanning (ALS) provides a non-invasive spatially- and structurally-explicit scaling mechanism between field-plot data and EC-based estimates of NEP within forest ecosystems. ALS biomass models typically utilize regression relationships between ALS canopy height profile metrics and plot-level biomass derived using allometric equations. In comparison with EC and plot data, ALS provides a one-time spatial characterisation of above-ground tree

biomass (Asner & Mascaro, 2014; Means et al., 1999; Næsset & Gobakken, 2008; Popescu, Wynne, & Nelson, 2003). For time intervals of three years or more, ALS has been demonstrated to accurately quantify canopy growth rates (Hopkinson, Chasmer, & Hall, 2008; Hudak et al., 2012; Næsset, Bollandsås, Gobakken, Gregoire, & Ståhl, 2013; Næsset & Gobakken, 2005) and biomass change (Økseter, Bollandsås, Gobakken, & Næsset, 2015; Skowronski, Clark, Gallagher, Birdsey, & Hom, 2014). It is feasible, therefore, to develop a framework that maps biomass C across the landscape, tracks changes through time and then reconciles these remote sensing observations with NEP.

Given the proliferation of large area, even nation-wide, ALS coverages in recent years (Wulder et al., 2012; Stoker, Cochrane, & Roy, 2013; Hopkinson et al., 2013) and new ecosystem monitoring programs like NEON and TERN in the USA and Australia, it is now logical and feasible to incorporate ALS within an integrated C flux monitoring framework. Indeed, this was a recommendation of a recent Fluxnet report (Beland et al., 2015). ALS is already a recognized method for better characterising flux tower site canopy structural variability (Chasmer et al., 2008b) within approximately 44 international Fluxnet sites, with at least 8 of these sites containing two or more temporal ALS datasets (Beland et al., 2015). Furthermore, the work of Chasmer et al. (2008a, 2008b and 2011) has provided the platform for such a framework by developing and refining methods of ALS forest canopy attribute integration with EC CO<sub>2</sub> flux data.

While an integrated EC and ALS ecosystem C monitoring framework is conceptually feasible, its implementation is challenged both as a result of: a) their currently being few sites around the world where long-term EC NEP records have been collected in tandem with multi-temporal ALS; and b) the subtle but critical differences in the way C pools and fluxes are quantified in EC, ALS and plot measurement methods. While plot-level monitoring can track changes in terrestrial C pools at distinct locations, this differs to ALS observations that can track above ground standing biomass changes across the landscape. And both are distinct to EC NEP, which is inferred from the NEE of C between the ecosystem and atmosphere within the footprint of a flux tower. Clearly then, each technique has distinct spatio-temporal domains of representation and each observes slightly different components of the terrestrial C cycle.

This paper addresses the disparate sampling and spatio-temporal representations of ALS, plot and EC ecosystem C observations and introduces a framework for data integration that, when combined, provides more information on ecosystem C balance than is possible using each method in isolation. The aim is to integrate all three approaches in a manner that accounts for and capitalises upon the different C pool and process representivity of each. A case study is presented to apply the integrated C assessment framework within a chronosequence of regenerating boreal forest stands over a six year period in an attempt to better partition GPP and NEP as the stands progress from adolescence to maturity.

## 2. Materials and methods

### 2.1. Study area

A chronosequence of four jack pine (*Pinus banksiana* Lamb.) stands, located approximately 100 km northeast of Prince Albert, Saskatchewan, Canada (53°54' N, 104°39' W, ~490 m a.s.l.) were examined in this study (Fig. 1). Jack pine is one of the most numerous boreal forest species, covering an area of ~517,000 km<sup>2</sup> of Canada and parts of the northern USA (Little, 1971), and therefore represents an important northern hemisphere component of global biomass. Two sites, a mature stand (91–97 year old; Old Jack Pine (OJP)) and an intermediate-aged stand harvested in 1975 (HJP75) were established during the Boreal Ecosystem Atmosphere Study (BOREAS) (Sellers et al., 1995) in 1993. Monitoring at the sites continued from 2001 to 2011 under the project name: Boreal Ecosystem Research and Monitoring Sites (BERMS) within

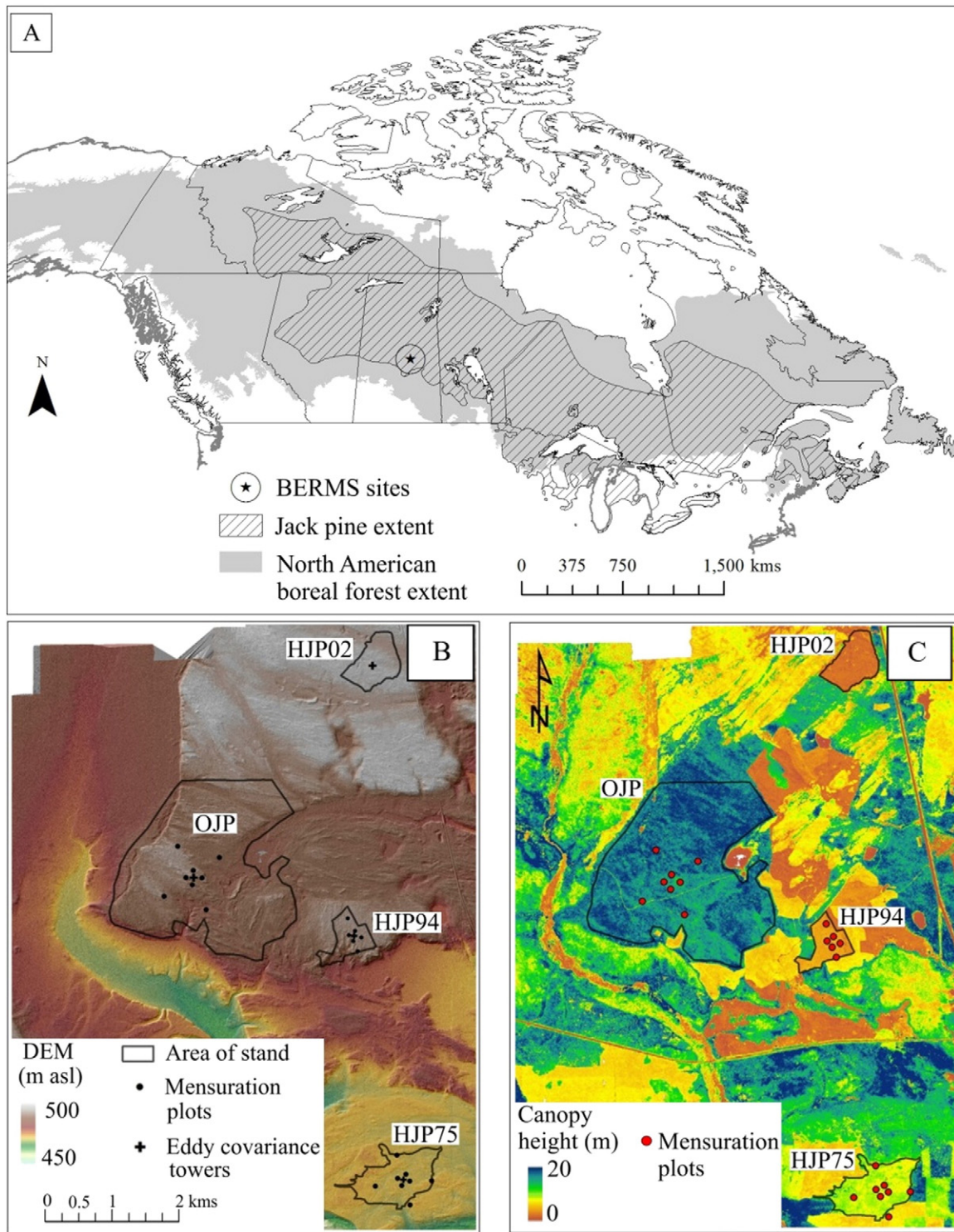


**Fig. 1.** A) Location of the jack pine chronosequence within the Canadian boreal forest [source: Brandt, 2009; region within which jack pine forests can be found is from Little (1971)]. Jack pine stand extents overlaid onto a: B) digital elevation model (DEM); and C) canopy height model (CHM). Field mensuration (FM) plot locations initiated in 2005 are also shown.

the Fluxnet Canada Research Network and the Canadian Carbon Program (Barr et al., 2004; Coursolle et al., 2006; Zha et al., 2013). Two additional jack pine stands, one harvested in 1994 (HJP94) and the other in 2002 (HJP02) were added to the existing BOREAS and Fluxnet Canada stands to complete the jack pine chronosequence (Fig. 1). Site characteristics are described in Zha et al. (2013). Soils at the sites are composed of glaciofluvial deposits, and are sandy and dry (Vogel & Gower, 1998). The sites have slightly undulating topography, with a maximum elevation variation of ~20 m within 1 km of the EC tower

at the OJP stand. In 2005, mean stand heights varied from 0.2 m to 14.2 m at HJP02 and OJP, respectively (Zha et al., 2013), with mean leaf area index ranging from  $0.3 \text{ m}^2 \text{ m}^{-2}$  to  $3.1 \text{ m}^2 \text{ m}^{-2}$  at HJP02 and HJP75, respectively (Chasmer et al., 2008a; Chen et al., 2006).

Long-term annual averages of minimum, mean, and maximum daily air temperatures for the nearest town site at Prince Albert, SK (~100 km south west) are  $-5.3 \text{ }^\circ\text{C}$ ,  $0.2 \text{ }^\circ\text{C}$ , and  $7.1 \text{ }^\circ\text{C}$ , respectively, while annual mean precipitation at Waskesiu Lake climate station (~100 km west) is ~467 mm (1981 to 2010 Environment Canada

climate normal). Slightly above normal total precipitation depths were observed throughout the period studied at Environment Canada's Waskesiu Lake climate station, with three-year means of 585 mm and 522 mm for 2005–2008 and 2008–2011, respectively. Air temperatures collected at the OJP flux tower indicate locally warmer conditions during 2005–2008 than 2008–2011, with mean growing season (April to September) temperatures of 13.0 °C and 12.5 °C, respectively. The study followed a period of drought from 2001 to 2003, during which local reductions were observed in ecosystem productivity (Kljun et al., 2007) and light use efficiency (LUE) (Chasmer et al., 2008a).

2.2. Conceptual framework

A simple conceptualisation of important terrestrial ecosystem C pools within a regenerating forest stand and their representation using different measurement methods is presented in Fig. 2 and provides the basis for the analysis presented. 'Understory' in Fig. 2 represents living shrubs, small trees and vegetation ground cover; 'litter' encompasses fine and coarse woody debris as well as decaying understory biomass; 'root' represents both fine and coarse components; 'soil' encompasses both organic and mineral components. C exchanges due to the import or export of inorganic sediments and animal movement is ignored or assumed to balance over long enough time periods. Dissolved Organic Carbon (DOC) is illustrated in Fig. 2 as it represents a potential C export. The brackets and text at right side of Fig. 2 illustrate how each measurement technique samples either an aggregate ecosystem C response through time (NEP) or distinct pools of C within the ecosystem (ALS and plots).

The implicit assumption in Fig. 2 is that if all terrestrial organic C pools can be monitored through time, then the change in total organic C ( $\Delta TC$ ) can be reconciled with NEP. Following Lovett et al. (2006):

$$NEP = \Delta TC + E + O_{x_{nb}} - I \tag{1}$$

where E represents exports of C, such as by harvest or by leaching of DOC; I represents imports, such as by animal movement or wind transport; and  $O_{x_{nb}}$  is the non-biological oxidation of C, which may occur as a result of fire or ultraviolet oxidation (Lovett et al., 2006). For the

purpose of this analysis, the BERMS sites are assumed balanced in terms of major imports and exports of organic C, and oxidation is considered a negligible component, as there have been no fires in these stands in recent decades. The most likely organic C export at the BERMS chronosequence would be DOC in groundwater but this has been shown to be a negligible component of the C balance with export values of  $\sim 0.002 \text{ tC ha}^{-1}$  (Grant et al., 2007). Therefore, we can formulate the following simple relationship:

$$NEP \approx \Delta TC = \Delta SLC + \Delta UC + \Delta RC + \Delta LC + \Delta SC. \tag{2}$$

Further, by assuming that the living understory and root components of a regenerating stand increase in biomass each year in concert with the standing living woody or tree biomass, we can estimate the understory and root C pools as a function of the generally larger standing live C pool (e.g. Kristensen et al., 2015):

$$(SLC + UC + RC) = f(SLC). \tag{3}$$

Then:

$$NEP \approx f(\Delta SLC) + (\Delta LC + \Delta SC). \tag{4}$$

Thus, NEP is equated to a function of the change in above ground live biomass that can be modelled from ALS, with a residual term that is associated with the changes in C storage within the litter and soil zone. The  $f(\Delta SLC)$  term represents the change in C within the total living biomass components (TLC) associated with tree stems, understory and roots and therefore:

$$\Delta TLC \approx NEP - (\Delta LC + \Delta SC). \tag{5}$$

This rearrangement facilitates a direct comparison of ecosystem C storage change estimates that can be generated from ALS and EC techniques. The litter, soil and export residual components of this C balance represent an important bulk quantity of forest ecosystem C store that can now be resolved.

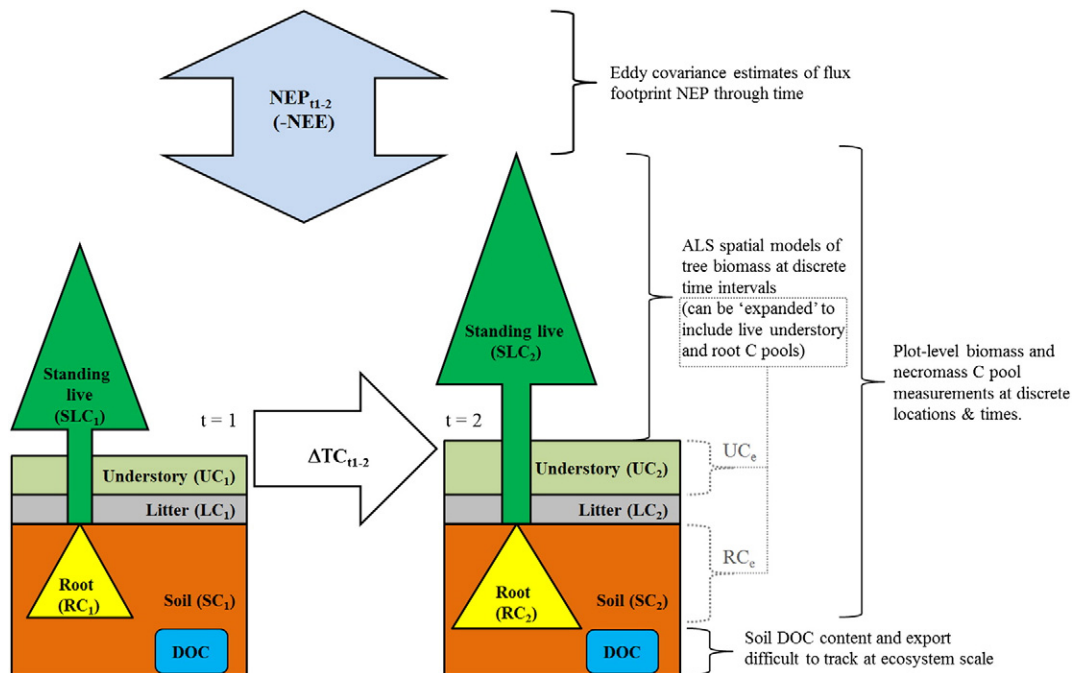


Fig. 2. A conceptual diagram illustrating how primary elements of ecosystem organic C in a regenerating forest can be tracked in time (t1 to t2) using eddy covariance, airborne laser scanning and C pool plots.

### 2.3. Eddy-covariance data

In this study, NEP = −NEE and GPP is determined from NEP minus ecosystem respiration (Re). Half-hourly fluxes of Atmospheric CO<sub>2</sub> (converted to tC ha<sup>−1</sup>) were measured at each of the jack pine chronosequence sites using standardized Fluxnet EC methods following Griffis et al. (2003), Barr et al. (2006) and Zha et al. (2013), and all data were corrected for energy balance closure (Barr et al., 2006; Barr et al., 2013). Due to the length of the study and remote nature of the sites, occasional instrument malfunction led to data gaps exceeding one year within three out of the four site datasets. Complete annual NEP measurements were available as follows: HJP02 (2003–2007); HJP94 (2001–2004; 2009–2011); HJP75 (2004–2007, 2010), and OJP (2000–2011; i.e. no inter-annual data gaps). While caution must be exercised with the interpretation of younger site NEP and GPP during data gap periods, two methods for filling these gaps were tested in order to construct cumulative NEP records: a) linear regression model between annual NEP and stand-age for periods when data exist; b) comparison of GPP and NEP from EC estimates with the GPP/PSN (photosynthesis, NPP) MODIS (MOD17A2\_5.1) data products downloaded from ([odaac.ornl.gov](http://odaac.ornl.gov)) for the tower pixel (Zhao, Heinsch, Nemani, & Running, 2005). Based on the results of this gap-filling comparison (presented below) and previous observations that NEP correlates well with stand-age (Zha et al., 2013), gap filling using the age-interpolation was ultimately chosen.

### 2.4. Plot biometric measurements

Two distinct types of field plots have been used in this study. The first are termed ‘forest mensuration plots’ (FM plots) and the second ‘C pool plots’ (CP plots). Both types made biomass measurements (detailed below) and utilised allometric equations to calculate tree and plot-level dry biomass in tC ha<sup>−1</sup> (Lambert, Ung, & Raulier, 2005). Dry biomass estimates were converted to C by assuming 50% of dry biomass is C (Atjay, Ketner, & Duvigneaud, 1977; Pregitzer & Euskirchen, 2004). FM plots of standing live biomass C (SLC<sub>plot</sub>) were used to calibrate an ALS model, while the purpose of the CP plots was to allow partitioning of the primary above- and below-ground biomass C pools so that the living biomass components of SLC, UC and RC could be related as per Fig. 2 and Eq. (3). Via this approach, ALS estimates of SLC could be expanded to account for all live biomass components (see below).

Coincident with the August 2005 ALS data collection (described below), eight, eight and six FM plots were set up at OJP, HJP75, and HJP94, respectively, for the explicit purpose of calibrating ALS forest attribute models (Chasmer et al., 2008b). The circular FM plots had radius of 11.3 m and were installed at radial distances of 100 m and 500 m (OJP, HJP75), and 100 m and 200 m (HJP94) from the flux towers at each site (Fig. 1). Plots were accurately located (<40 cm 95% CI) using >20 min rapid-static dual-frequency global positioning system (GPS) rover occupations relative to a GPS base station set over a fixed control marker in HJP02 < 10 km from each stand. Accurate FM plot location was critical to ensure field biomass data were precisely co-located with the ALS point cloud for subsequent SLC model construction. Measurements included diameter at breast height (DBH) and stem height for every tree with a DBH > 2 cm (Table 1). No ground cover or root biomass measurements were made at FM plots. Due to the immature regenerative state of HJP02 at the time of field visits (3 years after clear cut), biomass measurements were not collected at HJP02.

During the period 2005–2011, no CP plots were acquired but an archive of CP plot data from 1994 to 2004 was obtained: a) eight plots established in 1994 by Gower et al. (1997) at OJP and HJP75; b) five plots established in 1999 by Howard et al. (2004) at OJP, HJP75 and HJP94; c) three repeats of the Gower et al. (1997) OJP plots measured in 2004 by Theede (2007). As the CP plot data were collected across three historical studies, the range in available plot-level detail was variable. Raw data were available from Theede (2007), individual plot

summaries from Howard et al. (2004), and aggregate summaries from Gower et al. (1997).

It is known that the inter-relationship between living biomass components varies with age (e.g. Lehtonen, Makipaa, Heikkinen, Sievanen, & Liski, 2004; Peichl & Arain, 2007), so these plots, were used to develop a stand age-variant expansion factor (e) for total live biomass C (TLC) as a function of SLC. The locations of the CP plots are only approximately known but accurate positioning was not important, as they were not used in the calibration of ALS data. The e factor was derived as follows:

$$TLC = e \times SLC. \quad (6)$$

Following the above CP plot-level calculation, the resultant e factor was regressed against stand-age (a), to generate an age-variant e function, which was applied to SLC data derived from ALS in 2005, 2008 and 2011.

### 2.5. ALS data collection and processing

ALS data were collected during clear-sky conditions over each of the study sites in August 2005, 2008 and 2011 using a small-footprint multiple-discrete-return Airborne Laser Terrain Mapper (ALTM) 3100C (Teledyne Optech Inc., Toronto), operated with equivalent flight and sensor settings resulting in an aerial sampling density of >2 pts m<sup>−2</sup>. ALS point clouds were flight-line matched and classified into ground and non-ground returns using Terrascan (Terrasolid, Finland), and subsequently converted to 1 m raster triangulated irregular network digital elevation models (DEMs), localized maxima digital surface models (DSMs) and canopy height models (CHMs), which were the difference between the DEM and DSM. All raster grids were generated in Surfer (Golden Software, Denver, CO). CHM growth between data collections was estimated based on a 3 m × 3 m grid-size change in maximum height to reduce uncertainty due to small shifts in tree top position. Areal canopy cover losses, primarily associated with stem mortality, were illustrated at CHM grid nodes where the value had decreased by >2 m.

### 2.6. Estimating total living biomass C stocks from ALS

Standing live biomass C determined per 2005 FM plot (SLC<sub>plot</sub>), was used to construct ALS standing live biomass C (SLC<sub>ALS</sub>) models based on a variety of commonly used point cloud metrics described below. Point cloud data were first extracted within geo-registered 2005 FM plot extents and normalised to a height above ground-level by computing elevation residuals relative to the DEM. Point cloud metrics were derived on a per-plot basis and regressed against SLC<sub>plot</sub>. The following metrics were tested for all returns and all returns above 0.2 m (to remove ground influence and any near-ground noise in the data): mean, maximum, standard deviation, inter-quartile range (IQR), height percentiles [P25, P50, P75, P90, P95, P99] and the following ratios: i) all returns/all returns above 1.5 m, ii) all returns/all returns above average height, and iii) all returns/all first returns above 1.5 m. Single and dual variable linear, power, log and exponential models were tested. An optimal ALS model was chosen, based on predictive capability and consistency of its application to different datasets through time; i.e. if a model reproduced accurate plot-level biomass estimates for the year of plot and ALS sampling (2005) but produced noisy or biased biomass estimates when applied to 2008 or 2011, it was ignored. Temporal FM plot data were not available to test the ALS model in 2008 or 2011, so judgement was exercised based on field observations of canopy conditions at each site. For these reasons, if the explanatory power of a simple univariate or linear model was statistically equivalent to a more complex multivariate or non-linear model, then it was chosen; i.e. simplicity was preferred over complexity in the absence of more quantifiable decision criteria. The assumption is that a simpler technique may not always produce the highest accuracy model but it should be more

**Table 1**  
Summary of jack pine stand CP and FM plot measurements from four historical datasets.

Author	Gower et al. (1997)	Howard, Gower, Foley, and Kucharik (2004)	Theede (2007)	Chasmer et al. (2008b)
Year	1994	1999	1994, 2004	2005
Number of plots (type)	8 (CP)	5 (CP)	3 (CP)	22 (FM)
Plot size (m <sup>2</sup> ), shape	56 (HJP75), 625 (OJP), square	625, square	625, square	400, circle
Plot measurements	Tree number, DBH	Tree number, DBH	Tree number, DBH	Tree number, DBH, tree height, understory
Number of sub-plots	4	4	3	0
Sub-plot measurements	Destructive sampling of seedlings, shrubs, herbs, mosses, all oven-dried	Per Gower et al.	Per Gower et al.	N/A
Litter-traps	Periodically emptied and oven-dried	Per Gower et al.	Per Gower et al.	N/A
Mineral soil C content	Coarse roots, fine roots	coarse roots; 10 soil cores; fines	Per Gower et al.,	N/A
Coarse woody debris	10 m transects	10 m transects	10 m transects	N/A

robust for comparative analyses across a range of datasets containing diverse canopy heights and densities (e.g. Hopkinson, Chasmer, Lim, Treitz, & Creed, 2006).

Following selection of a suitable SLC<sub>ALS</sub> model, it was applied to the point clouds across the entire jack pine study area. Modelled data were gridded at 20 m × 20 m grid cell resolution to be equivalent in area to the 400 m<sup>2</sup> FM plots used in calibration and ensure adequate ALS returns (typically 600 to 1000 points) in each cell for percentile- or ratio-based model implementation. The previously derived expansion factor,  $e$ , was applied to SLC<sub>ALS</sub> grids per Eq. (6) to estimate total live biomass C (TLC<sub>ALS</sub>) across all stands for each year of ALS data (2005, 2008 and 2011). Confidence intervals (95% CI) were calculated to describe the range of rasterised jack pine TLC<sub>ALS</sub> variability in: a) 2005 mensuration FM plot locations (number of grid cells ( $n$ ) = 32 for HJP75 and OJP, and 24 at HJP94); and b) each stand ( $n > 10,000$  grid cells). The change in TLC<sub>ALS</sub> ( $\Delta$ TLC<sub>ALS</sub>) or net live biomass accumulation was calculated by differencing the grid models and summarising by stand and plot locations.

### 2.7. Footprint extraction

In order to compare spatial biomass changes mapped from remote sensing with flux-tower measurements of NEP, the two data types must be reconciled to a common spatial and temporal reference frame. This is achieved by modelling the spatial extent of the EC flux footprint for the time period of interest (Vesala et al., 2008; Leclerc & Foken, 2014). The flux footprint is defined as the probability of flux contribution per unit area upwind of EC instrumentation (Kljun, Calanca, Rotach, & Schmid, 2004; Kljun, Rotach, & Schmid, 2002; Schmid, 1994). A raster-based footprint parameterization based on Kljun et al. (2004) was used to map EC-sampled source/sink areas per half-hour period. Following the methods of Chasmer et al. (2011), the half-hourly footprints were then totalised over entire years to determine appropriate grid-cell weightings of  $\Delta$ TLC<sub>ALS</sub> around each of the EC towers. Footprint weighting provides the most spatially comparable estimate of  $\Delta$ TLC<sub>ALS</sub> to EC-based estimates of GPP and NEP. The year nearest to the 2008 ALS dataset collected at the midpoint of the time series was chosen (HJP94: 2009; HJP75: 2007; OJP: 2008) to represent median stand-level canopy structure conditions, which were necessary inputs for the footprint parameterization (Chasmer et al., 2008b and 2011). The 95% CI of the within-flux-footprint  $\Delta$ TLC<sub>ALS</sub> was calculated from all grid cells within the footprint probability density function 90% contour ( $n > 5000$  and varies with footprint extent).

### 2.8. Comparative analyses

As a test of plot-location stand representivity, samples of TLC<sub>ALS</sub> data were extracted for each of the FM plot locations (four grid cells per plot), summarised and compared to stand-level TLC<sub>ALS</sub>. Then stand- and plot-level TLC<sub>ALS</sub> estimates were compared for each of the stands and the three sample periods to quantify differences in total live biomass C

with stand-age. Due to close proximity and comparable soil conditions, it was assumed the stands do not differ significantly in terms of fertility or climatic inputs and thus their age is the primary control on their response to external drivers. A time-series of stand-level TLC<sub>ALS</sub> was plotted as a function of stand-age to visually assess whether or not the biomass accumulation trends at individual stands, were consistent with the chronosequence as a whole. CP plot estimates of TLC collected during the 11 years prior to the ALS missions were also included in this analysis for comparison, as they extended the age range represented.

The  $\Delta$ TLC<sub>ALS</sub> results were also compared with EC-based GPP at stand-level (for comparable years) and then with NEP at footprint-level (using gap filled data). A  $\Delta$ TLC<sub>ALS</sub>/GPP ratio is here considered an index of the efficiency with which C sequestered during photosynthesis has been stored in inter-annual total live biomass accumulation for each of the jack pine stands. For the purpose of this study, this ratio is referred to as live C use efficiency (LCUE). To further assess spatial sampling influences on biomass accumulation estimates, total live biomass accumulation ( $\Delta$ TLC<sub>ALS</sub>) at FM plot-locations, stands and within EC tower footprints were compared. Finally, the footprint-weighted  $\Delta$ TLC<sub>ALS</sub> data were subtracted from NEP to derive the residual (NEP –  $\Delta$ TLC<sub>ALS</sub>), which as per Eq. (5) represents the combination of changes in C storage in the litter and soil C pools ( $\Delta$ LC +  $\Delta$ SC). This last step partitions ecosystem C into more fundamental quantities than either ALS or EC methods can directly infer and, therefore, presents new information about the ecosystem C balance.

## 3. Results

### 3.1. Gap filling NEP

MODIS GPP overestimated EC GPP and correspondence was poor within younger sites requiring gap-filling, while the PSN product is not comparable to NEP estimated using eddy covariance methods and therefore was not used. Linear regression and interpolation between NEP and stand-age was, however, sufficient for use as an inter-annual NEP gap filling approach. OJP is the oldest of the sites and thus the least likely to demonstrate any relationship between annual NEP and stand age ( $r^2 = 0.04$ ). At HJP75, NEP is missing from 2008 to 2009, but for remaining years NEP increases linearly with age ( $r^2 = 0.70$ ). The gap at HJP94 (2005–2008) is bracketed by four years prior and three years following, and the age-dependent linear relationship was strong ( $r^2 = 0.92$ ). Missing data during years 2008–2011 at HJP02 (stand age of 6 to 9 years) were filled based on the linear regression of HJP02 NEP data from 2003 to 2007 and data from HJP94 (stand age 7 to 10 years) ( $r^2 = 0.86$ ). The proportions of gap-filled EC NEP data are 0% (OJP), 28% (HJP75), 36% (HJP94) and 44% (HJP02). Annual climatic variability may influence CO<sub>2</sub> uptake and biomass growth at jack pine chronosequence sites, especially during warm, dry years (Grant et al., 2007), but the influence of climate on annual NEP residuals from the age-variant linear regression trend at younger sites (HJP02, HJP94 and HJP75) is not found to be significant ( $p = 0.45$ ; 0.37 and 0.78,

respectively). Cumulative annual precipitation is within 23% of the 6-year average and average air temperatures are within 2 °C.

### 3.2. Growth and loss of jack pine from 2005 to 2011

The ALS CHM changes from 2005 to 2011 (Fig. 3) indicated annual canopy height growth rates (mean  $\pm$  1 s.d.) of  $0.09 \pm 0.70$  m  $y^{-1}$  at OJP;  $0.28 \pm 0.09$  m  $y^{-1}$  at HJP02;  $0.39 \pm 0.16$  m  $y^{-1}$  at HJP75; and  $0.63 \pm 0.22$  m  $y^{-1}$  at HJP94. While all stands displayed net vertical growth, areal loss of canopy cover (or increase in canopy gaps) over the 6-year period was <16% at OJP, and  $\leq$ 1% for younger stands. Minor tree stem or canopy cover losses within the OJP stand appear randomly distributed but mostly within 500 m of the EC tower. There are two noticeable clusters of canopy loss within or close to the periphery of the stand. One on the northwest side of OJP, adjacent to a small escarpment  $\sim$ 1 km from the flux tower, and another surrounding a small boreal pond  $\sim$ 1 km east of the tower. Other areas of canopy cover reduction are found north of HJP75 and south, east and west of the HJP02 stand. The large areas of loss surrounding HJP02 are due to post-harvest mortality and/or selective thinning.

### 3.3. Total live carbon estimates from airborne laser scanning

In 2005, FM plot-level standing live C ( $SLC_{plot}$ ) within the chronosequence ranged from  $0.8$  tC  $ha^{-1}$  at HJP94 to  $50.9$  tC  $ha^{-1}$  at OJP. Plot-level  $SLC_{ALS}$  regression model results are presented in Table 2. The most highly correlated univariate regression model was a power function of the average height of the 'all return' point-cloud distribution ( $Avg_{all}$ ) ( $r^2 = 0.98$ ,  $RMSE = 2.4$  tC  $ha^{-1}$ ,  $n = 22$ ). This model was not chosen, however, for the following reasons: i) it did not pass through the origin, resulting in physically impossible negative SLC predictions from plot data; ii) outside the height range of the training dataset,  $SLC_{ALS}$  increased unrealistically for small increases in  $Avg_{all}$ ; iii) when applied to 2008 and 2011 datasets, comparisons illustrated unrealistic changes in  $SLC_{ALS}$  over locations where biomass was accumulating at a relatively steady state. From Table 2, it is evident that simple linear models with zero origin produced model results that were comparable to non-linear models.

The optimal model based on regression results, temporal comparisons and physical basis was one using a scaling function of the all return point-cloud interquartile range ( $IQR_{all}$ ) ( $r^2 = 0.96$ ,  $RMSE = 3.2$  tC  $ha^{-1}$ ,  $n = 22$ ) (Fig. 4).  $IQR_{all}$  is an appropriate predictor of  $SLC_{plot}$  because it is

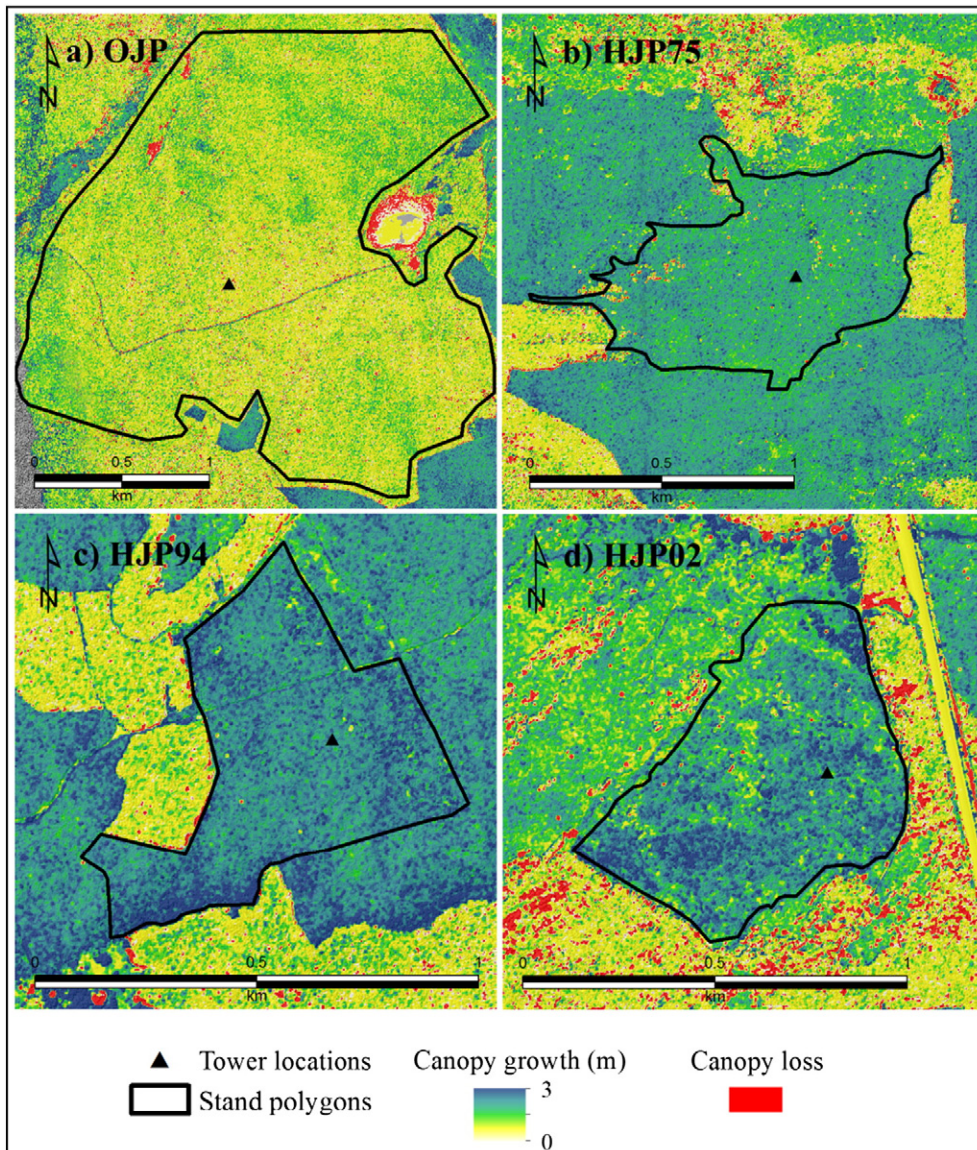


Fig. 3. Growth and loss of canopy between 2005 and 2011: a) OJP; b) HJP75; c) HJP94; and d) HJP02. Each scale bar is 1 km in length.

**Table 2**

Plot-level SLC<sub>ALS</sub> model results at the BERMS jack pine stands. (All models are significant for  $p < 0.05$ ), where P = percentile; Max = maximum height; Avg<sub>all</sub> = average height of all returns; SD = standard deviation of all returns; IQR<sub>all</sub> = interquartile range of all returns; All/1.5 = fractional cover of all returns/all returns above 1.5 m; and All/avg = fractional cover of all returns/all returns above average height.

Point-cloud metric	r <sup>2</sup> (all returns)		r <sup>2</sup> (all returns >0.2 m)	
	Linear model through origin	Non-linear model	Linear model through origin	Non-linear model
P25	0.41	0.53	0.45	0.79
P50	0.09	0.43	0.92	0.96
P75	0.96	0.97	0.94	0.94
P90	0.95	0.97	0.93	0.93
P95	0.94	0.96	0.92	0.93
P99	0.92	0.92	0.91	0.91
Max	0.9	0.91	0.9	0.91
Avg <sub>all</sub>	0.97	0.98	0.9	0.93
SD	0.95	0.96	0.91	0.91
IQR <sub>all</sub>	0.96	0.97	0.56	0.87
All/1.5	0.62	0.91	0.6	0.88
All/avg	0.34	0.75	0.24	0.81

an index of the overall ground to canopy point-cloud distribution height and density, and, unlike other percentile metrics, has low sensitivity to distribution tails.

The expansion factor  $e$  to convert SLC to TLC (Eq. (6)) is presented as an age-variant function in Fig. 5. One of two (HJP94), and two of three (HJP75) single stand measurement periods had  $e$  factors outside of the 95% confidence interval. While the data sources have been collected by different individuals and there is a possibility for variations in methodology and data quality (Table 1), it is clear that  $e$  decreases with increasing stand-age (Lehtonen et al., 2004; Peichl & Arain, 2007), approaching stabilization at OJP (Dickson, 1989; Tobin & Nieuwenhuis, 2007).

Applying the IQR<sub>all</sub> model of Fig. 4 to derive SLC, and expanding based on Eq. (6) and the function in Fig. 5 to derive TLC, results in the following expression:

$$TLC_{ALS} = 8.5 \times IQR_{all} \times a^{-0.131} \quad (7)$$

where (a) is stand-age (years). Applying Eq. (7) to the gridded IQR<sub>all</sub> ALS data for each of the four jack pine stands produces a spatially explicit map of total living biomass C across the landscape (Fig. 6). Note the spatial variability in TLC<sub>ALS</sub> across each of the stands. In particular, OJP tends to illustrate elevated biomass values at greater distances from the flux tower, while HJP75 and HJP94 both indicate lower biomass levels on the northeast side of the stands. Also note that TLC<sub>ALS</sub> for the

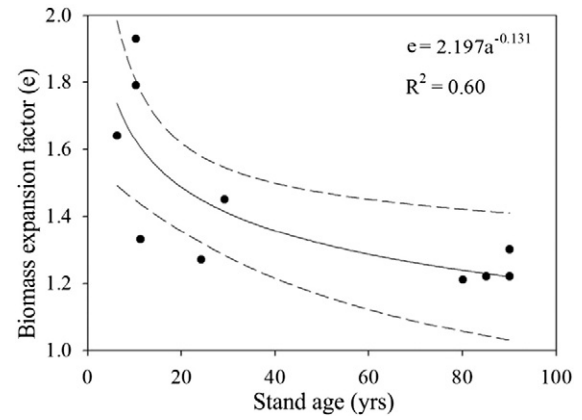


**Fig. 5.** Stand age-dependent biomass expansion function ( $e$ ) for comparable CP plot data (HJP94, HJP75 and OJP). Mean power-function trend line (solid line) and 5th/95th % confidence limits (dashed lines) are illustrated.

HJP02 stand (Fig. 6d) relied on extending the SLC<sub>ALS</sub> model (Fig. 4) to zero and extrapolating Eq. (7) outside the range of  $e$  factor observations (Fig. 5). Consequently, the uncertainties associated with the 2005 HJP02 TLC<sub>ALS</sub> estimates are indeterminate.

### 3.4. Comparisons between modelled live biomass, biomass accumulation and GPP

Stand-level TLC<sub>ALS</sub> was consistently greater than the mean plot-location estimates but were within the 95% confidence interval (Table 3). Proportional differences are greatest at HJP94, where stand biomass exceeds the plot mean by up to 26%. At OJP, stand estimates were consistently ~5 tC ha<sup>-1</sup> or ~10% higher than plot means. The greatest retention of C in biomass accumulation occurs in HJP94, followed by HJP75, while LCUE is smallest at the youngest and oldest stands.

Plotting mean stand-level TLC<sub>ALS</sub> against age for all stands and sample years produces a Sigmoidal growth trend (Fig. 7). Biomass accumulation rates are small up to approximately 10 years, then increase at the greatest rate between 10 and 30 years of age, and finally decrease as stands approach maturity. Field plot-level biomass TLC data (Howard et al., 2004; Theede, 2007; and the Fluxnet DIS archive) are comparable to ALS modelled estimates, except for OJP where the Howard et al. (2004) and Theede (2007) plots demonstrate a large negative deviation (>10 tC ha<sup>-1</sup>) from the Sigmoidal growth curve (Fig. 7). While there is no temporal overlap between these historical plot data, the 95% confidence limits in field plot data (80 to 90 years) and stand-level TLC<sub>ALS</sub> data (91 to 97 years) overlap, indicating the sample populations share common values at individual plot and grid cell-levels. Further, while the locations of these historical plots are not accurately known and cannot be directly compared to ALS results, it is known that they are close to the EC flux tower. As observed in Fig. 6, total biomass in the 500 m area surrounding the OJP tower is visibly lower (>5 tC ha<sup>-1</sup>) than most of the stand, so it is likely that a high proportion of the historical CP plot data represent areas containing lower biomass levels than the mean for the entire stand.

### 3.5. Comparing total live biomass accumulation with NEP

Flux footprint-weights and extents are illustrated over  $\Delta TLC_{ALS}$  for each of the three older stands in Fig. 8. Table 4 provides a summary of the FM plot-location, stand and footprint-weighted estimates of average annual total live biomass C accumulation and NEP at each site. Differences between plot, stand and footprint-weighted  $\Delta TLC_{ALS}$  (Table 4) are not significantly different (based on a paired two-sample  $t$ -test for means). Greatest similarity exists between plot- and footprint-level  $\Delta TLC_{ALS}$  ( $p = 0.38$ ), while larger differences are found between plot-

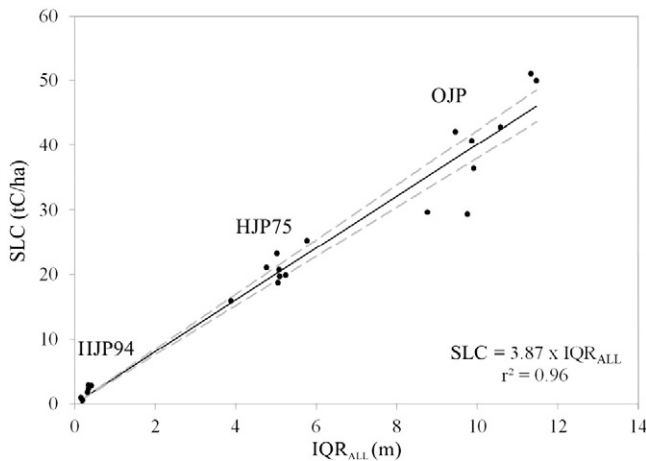


**Fig. 4.** Optimal single variable linear regression model of FM plot-level standing live C from the ALS point-cloud inter-quartile range of all returns (IQR<sub>ALL</sub>). Dashed lines are 5th/95th % confidence limits.

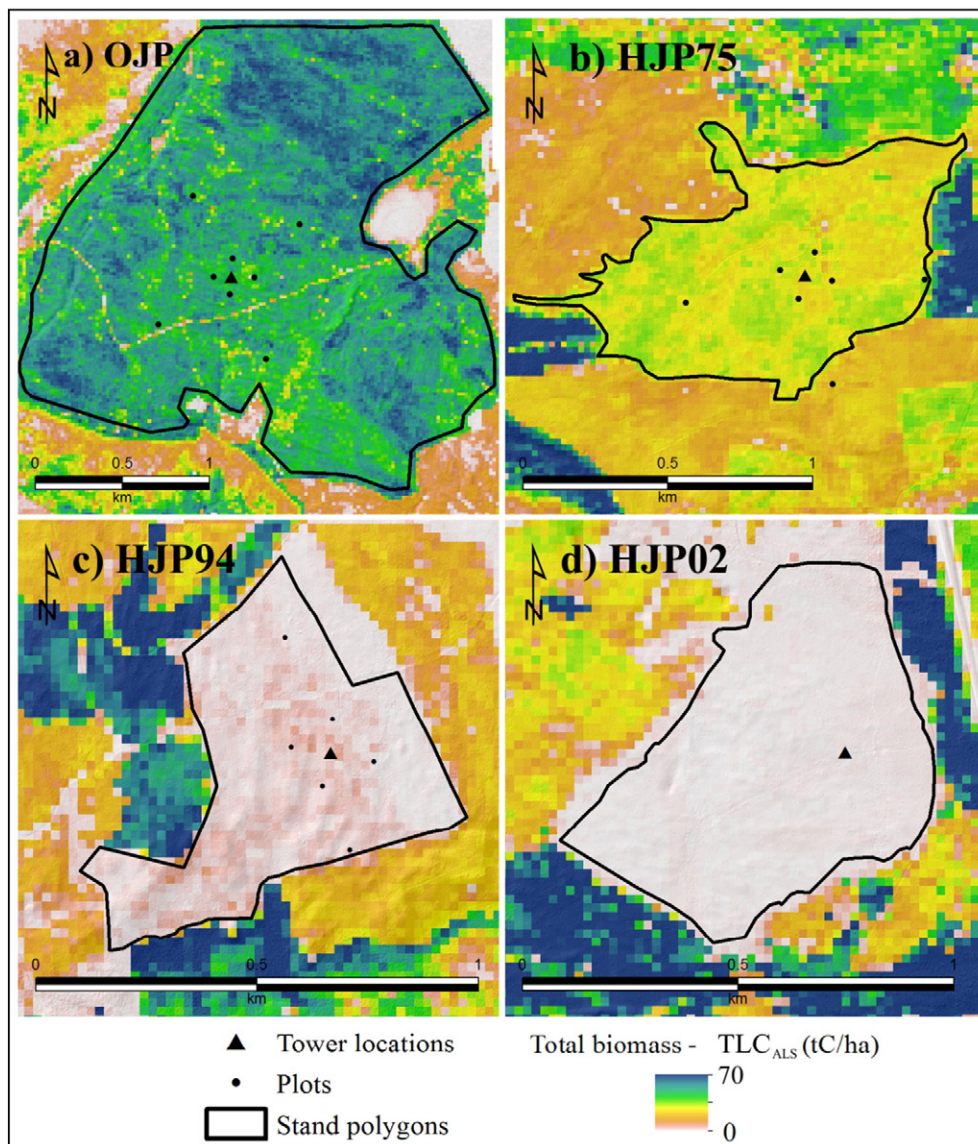


Fig. 6. Spatially explicit map of  $TLC_{ALS}$  for the jack pine chronosequence stands in 2005. Each scale bar is 1 km in length.

and stand-level ( $p = 0.12$ ) and between stand- and footprint-level ( $p = 0.15$ ). When comparing footprint-weighted  $\Delta TLC_{ALS}$  with average NEP, the differences for each stand exceed the 95% CI in NEP but are not in themselves significant at the 95% level of confidence ( $p = 0.18$ ). This demonstrates that a high proportion of NEP is captured in the ALS-based model of total live biomass C accumulation.

The change in total live C estimated from footprint-weighted  $\Delta TLC_{ALS}$  demonstrates a higher rate of C accumulation in biomass than average NEP at the immature HJP94 and HJP75 stands, whereas at the mature OJP stand the opposite occurs (Table 4 and Fig. 9). The residual component,  $NEP - \Delta TLC_{ALS}$  (described in Eq. (5)), represents the change in soil and litter C storage ( $\Delta SC + \Delta LC$ ) associated with

**Table 3**  
BERMS stand- and FM plot-location  $TLC_{ALS}$  estimates and the associated differences between years surveyed. Also shown is the LCUE ratio of  $\Delta TLC_{ALS}$  to mean GPP for the study period (GPP periods vary due to data availability).

Stands	Mean $TLC_{ALS}$ ( $tC\ ha^{-1}$ ) ( $\pm 95\%$ CI)			$\Delta TLC_{ALS}$ ( $tC\ ha^{-1}$ )			$\Delta TLC_{ALS}/GPP$
	2005	2008	2011	2005–08	2008–11	2005–11	%GPP
HJP02	N/A	0.35 ( $\pm 0.03$ )	1.00 ( $\pm 0.09$ )	N/A	0.7	N/A	1%
HJP94	1.80 ( $\pm 0.16$ )	7.00 ( $\pm 0.67$ )	13.76 ( $\pm 1.38$ )	5.2	6.8	12.0 ( $\pm 1.6$ )	34%
HJP75	28.93 ( $\pm 3.27$ )	30.86 ( $\pm 3.56$ )	34.42 ( $\pm 4.03$ )	1.9	3.6	5.5 ( $\pm 1.7$ )	10%
OJP	54.47 ( $\pm 7.52$ )	54.94 ( $\pm 7.63$ )	55.87 ( $\pm 7.80$ )	0.5	0.9	1.4 ( $\pm 3.2$ )	4%
Plots							
HJP94	1.65 ( $\pm 0.25$ )	5.54 ( $\pm 0.86$ )	11.83 ( $\pm 1.75$ )	3.9	6.3	10.2	25%
HJP75	28.34 ( $\pm 4.43$ )	30.50 ( $\pm 4.87$ )	33.96 ( $\pm 5.60$ )	2.2	3.5	5.6	12%
OJP	49.58 ( $\pm 8.17$ )	50.30 ( $\pm 8.54$ )	51.15 ( $\pm 8.44$ )	0.7	0.9	1.6	9%

<sup>a</sup> Eddy-covariance (EC) data availability varies per year and per site. Ratios are for periods when there were EC data.

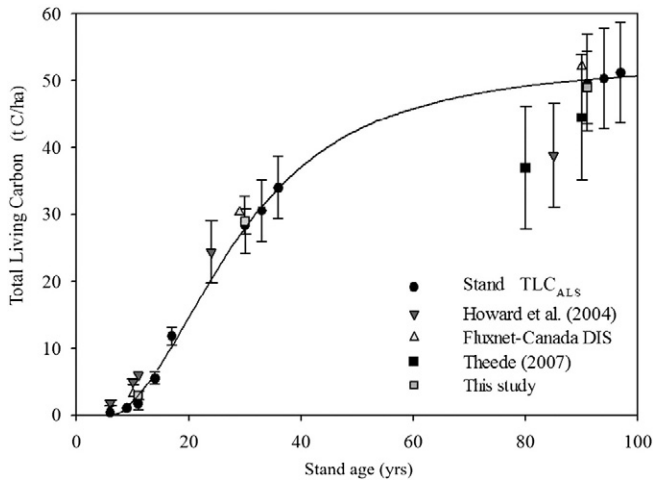


**Fig. 7.** Total live biomass (TLC<sub>ALS</sub>) accumulation with stand age for the jack pine chronosequence, with comparable plot-level summaries. Error bars represent 95% confidence limits for field plot or stand-level data. [Note: Sigmoid curve plotted through stand TLC<sub>ALS</sub> data only ( $n = 11$ ,  $r^2 = 0.99$ ).]

necromass C. The interpolated curve in Fig. 9, therefore, suggests the soil and litter C pools are a source of ecosystem C in immature stands and a sink of C in older stands.

**4. Discussion**

**4.1. Plot location and within site representivity**

Stand-level estimates of TLC<sub>ALS</sub> were greater than mean plot-location estimates at all sites (Table 3). These differences suggest that the FM plots chosen in 2005 to be within the EC flux footprints, while distributed on a pre-determined radial grid up to 500 m from the flux towers (Fig. 1), have systematically over-represented areas of slightly lower biomass ( $>5 \text{ tC ha}^{-1}$ ) than is typical across the complete stand area. This does not invalidate the ALS models, as the plots represent the range of biomass experienced in the stands but it does illustrate that aggregate plot-based estimates of biomass may not characterise the spatial domain they are assumed to represent. This is further illustrated in Fig. 7, where the CP plot estimates of total live biomass C fall below the more spatially explicit ALS estimates.

Furthermore, the CP plots sampled for OJP by Gower et al. (1997); Howard et al. (2004) and Theede (2007) were from  $25 \text{ m} \times 25 \text{ m}$  square plots that were revisited by different teams. This suggests two additional factors: i) geometry dictates that unless corner positions, angles and side lengths are accurately surveyed there is a possibility of systematic under-estimation of the area. Even if all side lengths are accurately measured, if any corners  $\neq 90^\circ$  the area will be smaller than that of a perfect square. Similarly, if side lengths are measured along a ground slope instead of horizontally, a systematic areal under-estimate will occur. Therefore, the most likely error in the establishment of a square plot is

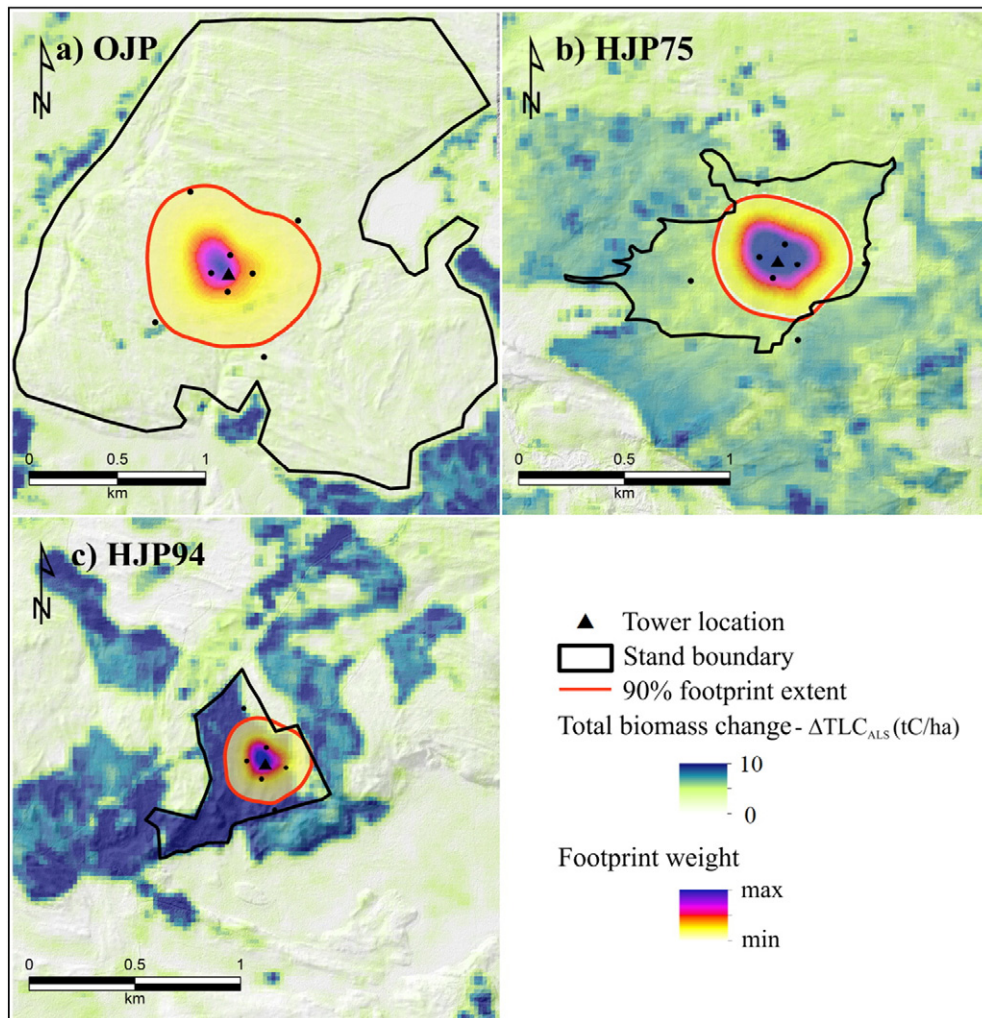


**Fig. 8.** Total live biomass accumulation ( $\Delta\text{TLC}_{\text{ALS}}$ ) from 2005 to 2011 for the three older jack pine stands. The 90th percentile cumulative extent and relative concentration weighting of the annual flux footprint is presented. [Note: HJP02 is not included, as biomass could not be accurately modelled for 2005.]

**Table 4**  
Annual live biomass accumulation ( $\Delta\text{TLC}_{\text{ALS}}$ ) at FM plot-locations, stands and within footprints, ( $\pm 95\%$  CI from mean in brackets) compared with mean annual NEP using EC methods and biomass accumulation residual ( $\text{NEP} - \Delta\text{TLC}_{\text{ALS}}$ ).

Sites	Stand age (years)	Mean annual change in biomass ( $\text{tC ha}^{-1} \text{yr}^{-1}$ ) (95% CI)			Mean NEP ( $\text{tC yr}^{-1}$ ) (95% CI)	NEP - $\Delta\text{TLC}_{\text{ALS}}$ ( $\text{tC ha}^{-1} \text{yr}^{-1}$ )
		Plot locations	Stands	Footprints		
HJP94	11–17	1.65 (+0.27, -0.33)	2.25 (+0.82, -2.09)	1.54 (+0.45, -0.77)	0.88 (0.36) <sup>a</sup>	-0.66
HJP75	30–36	0.84 (+0.18, -0.27)	1.05 (+0.23, -0.24)	0.90 (+0.18, -0.20)	0.63 (0.14) <sup>b</sup>	-0.27
OJP	91–97	0.32 (+0.30, -0.31)	0.35 (+0.41, -0.35)	0.32 (+0.40, -0.32)	0.45 (0.13) <sup>c</sup>	0.13

<sup>a</sup> HJP94: NEP data collected from 2001 to 2004, 2009–2011; missing from 2005 to 2008. Gap filling from 2005 to 2008 based on linear regression between years with data ( $r^b = 0.92$ ).

<sup>b</sup> HJP75: NEP data collected from 2004 to 2007, 2010; missing in 2008–2009, 2011. NEP estimated based on linear regression from available data used to gap fill years with missing data ( $r^2 = 0.70$ ).

<sup>c</sup> OJP: NEP data are complete for all years of study. OJP NEP is least influenced by stand age ( $r^2 = 0.04$ ).

to underestimate area and total biomass; ii) in observations analogous to Heisenberg's Uncertainty Principle (Heisenberg, 1927), Cahill et al. (2001) found that repeat vegetation plot measurements altered plant structure and impacted rates of herbivory. In a similar study by Semboli et al. (2014), it was found species composition in permanent sample plots varied as a result of repeat measurements. Since the establishment of BOREAS in 1993, there has been many data collection and equipment installation visits to the region surrounding the flux towers. While it is not known if either of the above factors has impacted biomass levels, the possibility of systematically reduced biomass estimates in historical plot data (as observed in Fig. 7) cannot be discounted. Similarly to the FM plots, this does not invalidate the use of the CP plots for biomass expansion factor development but it does indicate that it is not advisable to extrapolate ecosystem estimates of total biomass C from a small number of plots, while further supporting the implementation of non-invasive sampling techniques such as ALS.

#### 4.2. Biomass growth and carbon accumulation

Total live biomass accumulation ( $\text{TLC}_{\text{ALS}}$ ) over the six years at the stand-level was  $12.0 (\pm 1.6) \text{ tC ha}^{-1}$  at HJP94,  $5.5 (\pm 1.7) \text{ tC ha}^{-1}$  at HJP75, and  $1.4 (\pm 3.2) \text{ tC ha}^{-1}$  at OJP, indicating reduced biomass accumulation with stand age. However, biomass accumulation was slightly greater at these three sites between 2008 and 2011, relative to 2005–2008 (Table 3). Given the accelerated growth expected at HJP94 as the young stand ages (Fig. 7), this is to be expected. However, HJP75 and OJP also demonstrated increased growth increment in the latter period despite both stands being beyond the age of accelerating growth as inferred from the growth curve (Fig. 7). Despite the warmer and wetter conditions in the earlier period, reduced biomass accumulation during

this time could be a function of tree physiological recovery from the extended drought conditions from 2001 to 2003 (Chasmer et al., 2008; Kljun et al., 2007). For example, it is known that for the boreal forest species, Norway Spruce (*Picea abies*, L.), upper stem tree ring width and height increment can take three to four years to recover following an extended drought (Montwé, Spiecker, & Hamann, 2014).

When all chronosequence data are combined (Fig. 7), a sigmoidal growth relationship between total living biomass C and stand-age is evident. This characteristic growth function has been observed in numerous studies where young stands tend to have less biomass than mature stands, but higher NEP, depending on time since disturbance and recent history (Bhatti, Apps, & Jiang, 2002; Jandl et al., 2007; Kurz & Apps, 1999). In mature stands, growth rates decline to the point of stabilization, which occurs between approximately 80–200 years, depending on species type and past disturbance (Pregitzer & Euskirchen, 2004; Van Tuyl, Law, Turner, & Gitelman, 2005). At this development stage, C inputs into the ecosystem approximate C losses, resulting in low rates of C sequestration and minimal growth (Chapin et al., 2009).

#### 4.3. Live carbon use efficiency (LCUE)

The fraction of GPP captured and stored in live biomass accumulation was lowest within HJP02 and OJP (1% and 4%, respectively), and greatest within the rapidly growing HJP94 (34%) (Table 3). Comparable results were found in Peichl, Brodeur, Khomik, and Arain (2010) within a temperate afforested white pine (*Pinus strobus*, L.) chronosequence. From their estimate of ecosystem C use efficiency, which they defined as  $\text{CUE} = \text{NEP} / \text{GPP}$ , they found that middle-aged stands were more efficient at sequestering C than the youngest and oldest stands. Data in Table 3 and Peichl et al. (2010) suggest that in young pine stands experiencing high mortality due to competition and self-thinning, and in old stands where GPP is used for biomass maintenance, cumulative annual woody biomass increases are small relative to seasonal biomass production and replacement. However, while the observations are consistent, it is important to note that LCUE and CUE are parallel concepts but not equivalent. LCUE considers ecosystem C accumulation in living biomass only, whereas CUE considers all ecosystem inputs and outputs of organic C including soil exchanges.

#### 4.4. Soil carbon storage

The levelling off of jack pine biomass accumulation in Fig. 7 occurs beyond ~60 years, broadly coinciding with the age at which the difference between NEP and  $\Delta\text{TLC}_{\text{ALS}}$  reduces to zero (Fig. 9). This difference primarily represents changes in C storage within the litter ( $\Delta\text{LC}$ ) and soil ( $\Delta\text{SC}$ ) pools. From Fig. 9, the apparent trend in  $\text{NEP} - \Delta\text{TLC}$  (or  $\Delta\text{LC} + \Delta\text{SC}$ ) is characteristic of the soil C dynamics curve (Covington, 1981), and becomes more positive with stand age. This suggests that within a certain range of stand-age, the litter and soil storages transition from a net source to a net sink of ecosystem C. These observations shed new light on the C balance properties within the jack pine chronosequence at BERMS but are not unusual or unexpected results.

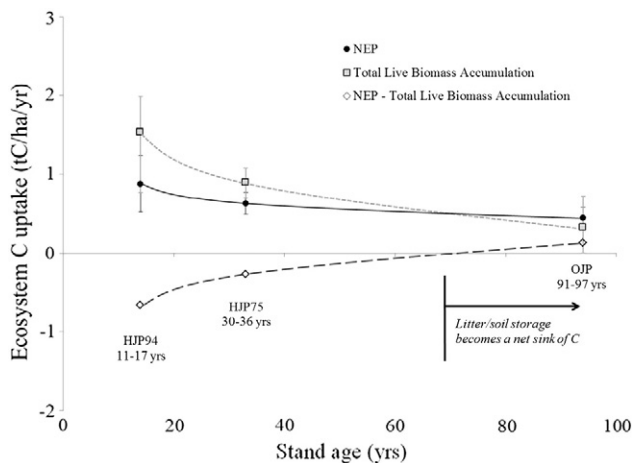


**Fig. 9.** Trends in average annual NEP and biomass accumulation for jack pine stands at different levels of maturity. The two components estimated directly are NEP from EC data and total live biomass accumulation ( $\Delta\text{TLC}_{\text{ALS}}$ ) modelled from plot-calibrated ALS data. The residual difference is primarily a measure of the change in C storage in the soil and litter zone. [Error bars = 95% CI].

Following Covington (1981); Lal (2005) found that soil C content declines sharply through the first ~20 years following harvest as a result of lower above-ground biomass, decreasing litter inputs, and changes in localized micro-climate. At HJP02, Howard et al. (2004) found that forest floor C content was 2–3 times greater immediately after harvest than the more mature jack pine stands, while Bhatti et al. (2002) and Kurz et al. (2013) suggest that harvesting creates a large input of coarse woody debris and accelerated decomposition due to reduced foliage cover and soil warming. Further corroboration is found in several studies illustrating that below-ground necromass C allocations decrease with increasing stand age (Law et al., 2001; Litton, Ryan, & Knight, 2004; Litton, Raich, & Ryan, 2007; Ryan, Binkley, Fownes, Giardina, & Senock, 2004; Peichl & Arain, 2007).

#### 4.5. Expansion factor limitations

The weakest link in the workflow presented is the expansion factor analysis required to relate SLC to TLC. Based on the model in Fig. 5 and the mean age of the stands during this study, SLC is expanded by ~20% ( $\pm 30\%$  at 95% CI) for OJP and ~55% ( $\pm 15\%$ ) for HJP94. These values were constructed from a small number (10) of independent or aggregated CP plot data that likely did not sample the full range of nutrient, age and growth characteristics across each stand. Consequently, more spatially representative plots might increase the 95% CI illustrated in Fig. 5 and propagated into Fig. 9. However, the outliers in Fig. 5 and small sample number have already resulted in a large 95% CI, and this is likely due to the CP plots being collected by different individuals over an 11 year period and using slightly different sample configurations. There may be some compensating effect of these two opposing influences but it is conceivable that the function in Fig. 5 possesses some bias or the 95% CI generated may not be a true estimate of model uncertainty. Nonetheless, compounding the uncertainty from Fig. 5 into the NEP and biomass accumulation comparison in Fig. 9 would further reduce confidence in the illustrated proximity of NEP and biomass accumulation components. This would impact the timing at which the soil and litter store becomes a C sink but would not change the overall trend of a transition from C source to sink. Given biomass expansion factors and their associated uncertainty are critical in quantifying the magnitude and reliability of  $\Delta\text{TLC}$ , it is recommended that the calculation and use of expansion factors in ALS biometry receive serious attention in any future use or refinement of the framework presented.

## 5. Conclusion

The study has presented a novel integration of diverse datasets, each able to record key components of ecosystem C balance in a forest environment. A boreal jack pine forest chronosequence was studied here but the approach is valid for any regenerating forest ecosystem where: i) EC data are available to provide cumulative estimates of  $\text{CO}_2$  flux, NEP and spatial footprint weightings of ecosystem flux source; ii) plot data are available to calibrate remote sensing biomass products and construct C pool expansion factors; and iii) temporal ALS (or other high resolution 3D data such as derived from terrestrial laser scanning (TLS) or unmanned airborne vehicle (UAV) platforms) to model the spatio-temporal variation in, and accumulation of, total living biomass C.

Integrating these C assessment techniques does not, at this time, result in 'standard' or widely used ecosystem C terms like Net Primary Production (NPP) or Carbon Use Efficiency (CUE); which is typically the ratio of NPP/GPP or sometimes NEP/GPP (e.g. Peichl et al., 2010). However, by combining spatially explicit measurements of ecosystem live biomass C accumulation with EC-based GPP and NEP, new realisations of ecosystem C dynamics are assessed. In particular, through live carbon use efficiency (LCUE), the connection between GPP and total live biomass accumulation (or growth) becomes explicit. This increases the synergy between the fields of atmospheric and ecosystem C

assessment, and national or commercial forest inventory monitoring, as it provides a framework to integrate timber growth and yield, ALS-based forest inventory and flux data to produce C metrics that are meaningful to stakeholders from many backgrounds.

Assessing the necromass C balance in detritus and soil organic C is typically invasive, can be highly spatially variable and cannot be easily quantified using non-invasive techniques. However, the framework presented improves our understanding of forest C dynamics, as in addition to directly observing above-ground biomass and NEP, it can indirectly measure the combined litter and soil C trajectory. High resolution remote sensing time series data and EC technologies are becoming simpler to obtain and more cost-effective. Furthermore, new satellite missions, such as NASA's GEDI (Global Ecosystem Dynamics Investigation) and ICESat (Ice Cloud Elevation Satellite) II or ESA's Biomass, will soon be enhancing our capacity to monitor 3D biomass change over large areas so novel methods that integrate in situ and orbital image-derived time-series data are needed. Consequently, there is great potential to test and refine similar integrated C assessment workflows in different ecosystem and data contexts. It is suggested that, ecosystem C monitoring and assessment programs should be designed explicitly to capitalise upon the differences and complementarities in remote sensing, in situ and atmospheric flux observations that have been highlighted and reconciled through this study.

## Acknowledgements

We acknowledge prior research and data collection by S. Gower (and group), E. Howard (and group) and A. Theede for archived field plot data. Eva van Gorsel, CSIRO is gratefully acknowledged for early discussions of the analysis and model presented. Data collection assistance in 2005 was provided by Chris Beasy and Bruce Davidson. ALS data collection was coordinated through the Canadian Consortium for Lidar Environmental Applications Research with funding and support from Environment Canada, Natural Resources Canada and the UK Natural Environment Research Council (NERC, Grant NE/G000360/1). EC measurements at the jack pine sites and archival of the FluxNet data information system (DIS) were supported by the Meteorological Service of Canada, the Fluxnet-Canada Research Network, and the Canadian Carbon Program. C. Hopkinson acknowledges funding support from the Natural Sciences and Engineering Council (NSERC) Discovery Grants Program (2015-06463). The authors declare no conflicts of interest.

Maps. KMZ file containing the Google maps of the most important areas described in this article.

## Appendix A. Supplementary data

Supplementary data associated with this article can be found in the online version, at doi: <http://dx.doi.org/10.1016/j.rse.2016.04.010>. These data include the Google maps of the most important areas described in this article.

## References

- Asner, G., & Mascaro, J. (2014). Mapping tropical forest carbon: Calibrating plot estimates to a simple LiDAR metric. *Remote Sensing of Environment*, 140, 614–624.
- Atjay, G. L., Ketner, P., & DuVigneaud, P. (1977). Terrestrial primary production and phytomass. In B. E. Bolin, T. Degen, S. Kempe, & P. Ketner (Eds.), *The global carbon cycle* (pp. 129–181). New York: John Wiley.
- Barford, C. C., Wofsy, S. C., Goulden, M. L., Munger, J. W., Hammond, E., Pyle, S. P., ... Moore, K. (2001). Factors controlling long- and short-term sequestration of atmospheric  $\text{CO}_2$  in a mid-latitude forest. *Science*, 294, 1688–1690.
- Barr, A. G., Morgenstern, K., Black, T. A., McCaughey, J. H., & Nesic, Z. (2006). Surface energy balance closure of the eddy-covariance method above three boreal forest stands and implications for the measurement of  $\text{CO}_2$  flux. *Agricultural and Forest Meteorology*, 140(1–4), 322–327.
- Barr, A. G., Richardson, A. D., Hollinger, D. Y., Papale, D., Arain, M. A., Black, T. A., ... Schaeffer, K. (2013). Use of change-point detection for friction-velocity threshold evaluation in eddy-covariance studies. *Agricultural and Forest Meteorology*, 171–172, 31–45.

- Barr, A., Black, T. A., Hogg, E. H., Griffis, T. J., Morgenstern, K., Kljun, N., ... Nestic, Z. (2007). Climatic controls on the carbon and water balances of a boreal aspen forest. 1994–2003. *Global Change Biology*, 13(3), 561–576.
- Barr, A. G., Black, T. A., Hogg, E. H., Kljun, N., Morgenstern, K., & Nestic, Z. (2004). Interannual variability in the leaf area index of a boreal aspen–hazelnut forest in relation to net ecosystem production. *Agricultural and Forest Meteorology*, 126, 237–255.
- Beland, M., Parker, G., Harding, D., Hopkinson, C., Chasmer, L., & Antonarakis, A. (2015). White paper – On the use of LiDAR at AmeriFlux sites. (Available online at: <http://ameriflux.lbl.gov/resources/reports/>; AmeriFlux Publication, Lawrence Berkeley National Laboratory. 33 pp. Last accessed January 2016).
- Bhatti, J. S., Apps, M. J., & Jiang, H. (2002). Influence of nutrients disturbances and site conditions on carbon stocks along a boreal forest transect in central Canada. *Plant and Soil*, 242, 1–14.
- Brandt, J. P. (2009). The extent of the North American boreal zone. *Environmental Reviews*, 17, 101–161.
- Cahill, J. F., Jr., Castelli, J. P., & Casper, B. B. (2001). The herbivory uncertainty principle: Visiting plants can alter herbivory. *Ecology*, 82(2), 307–312.
- Canadell, J. G., Kirschbaum, M. U. F., Kurz, W. A., Sanz, M. -J., Schlamadinger, B., & Yamagata, Y. (2007). Factoring out natural and indirect human effects on terrestrial carbon sources and sinks. *Environmental Science & Policy*, 10, 370–384.
- Chapin, F. S., III, McFarland, J., McGuire, D., Euskirchen, E. S., Ruess, R. W., & Kielland, K. (2009). The changing global carbon cycle: Linking plant–soil carbon dynamics to global consequences. *Journal of Ecology*, 97(5), 840–850. <http://dx.doi.org/10.1111/j.1365-2745.2009.01529.x>.
- Chasmer, L., Kljun, N., Barr, A., Black, A., Hopkinson, C., McCaughey, H., & Treitz, P. (2008b). Vegetation structural and elevation influences on CO<sub>2</sub> uptake within a mature jack pine forest in Saskatchewan, Canada. *Canadian Journal of Forest Research*, 38, 2746–2761. <http://dx.doi.org/10.1139/X08-121>.
- Chasmer, L., Kljun, N., Hopkinson, C., Brown, S., Milne, T., Giroux, K., ... Petrone, R. (2011). Characterizing vegetation structural and topographic characteristics sampled by eddy covariance within two mature aspen stands using lidar and a flux footprint model: Scaling to MODIS. *Journal of Geophysical Research – Biogeosciences*, 116(G2). <http://dx.doi.org/10.1029/2010JG001567>.
- Chasmer, L., McCaughey, H., Barr, A., Black, A., Shashkov, A., Treitz, P., & Zha, T. (2008a). Investigating light-use efficiency across a jack pine chronosequence during dry and wet years. *Tree Physiology*, 28(9), 1395–1406.
- Chen, J. M., Govind, A., Sonnentag, O., Zhang, Y., Barr, A., & Amiro, B. (2006). Leaf area index measurements at Fluxnet-Canada forest sites. *Agricultural and Forest Meteorology*, 140(1–4), 257–268.
- Ciais, P., Reichstein, M., Viovy, N., Granier, A., Ogee, J., Allard, V., ... Valentini, R. (2005). Europe-wide reduction in primary productivity caused by the heat and drought in 2003. *Nature*, 437(7058), 529–533.
- Coursolle, C., Margolis, H. A., Barr, A. G., Black, T. A., Amiro, B. D., McCaughey, J. H., ... Hedstrom, N. (2006). Late-summer carbon fluxes from Canadian forests and peatlands along an east-west continental transect. *Canadian Journal of Forest Research*, 36(3), 783–800.
- Covington, W. (1981). Changes in forest floor organic matter and nutrient content following clear cutting in northern hardwoods. *Ecology*, 62(1), 41–48.
- Curtis, P. S., Hanson, P. J., Bolstad, P., Barford, C., Randolph, J. C., Schmid, H. P., & Wilson, K. B. (2002). Biometric and eddy-covariance based estimates of annual carbon storage in five eastern North American deciduous forests. *Agricultural and Forest Meteorology*, 113, 3–19.
- Dickson, R. E. (1989). Carbon and nitrogen allocation in trees. *Forest Science*, 46, 631–647.
- Gower, S. T., Vogel, J. G., Norman, J. M., Kucharik, C. J., Steele, S. J., & Stow, T. K. (1997). Carbon distribution and aboveground net primary production in aspen, jack pine, and black spruce stands in Saskatchewan and Manitoba, Canada. *Journal of Geophysical Research*, 102(D24), 29,029–29,041.
- Grant, R. F., Barr, A. G., Black, T. A., Gaumont-Guay, D., Iwashita, H., Kidson, J., ... Saigusa, N. (2007). Net ecosystem productivity of boreal jack pine stands regenerating from clearcutting under current and future climates. *Global Change Biology*, 13(7), 1423–1440.
- Griffis, T. J., Black, T. A., Morgenstern, K., Barr, A. G., Nestic, Z., & Drewitt, G. B. (2003). Eco-physiological controls on the carbon balances of three southern boreal forests. *Agricultural and Forest Management*, 117, 53–71.
- He, L., Chen, J. M., Pan, Y., Birdsey, R., & Kattge, J. (2012). Relationships between net primary productivity and forest stand age in U.S. forests. *Global Biogeochemical Cycles*, 26, GB3009.
- Heisenberg, W. (1927). Über den anschaulichen Inhalt der quantentheoretischen kinematik und mechanik. *Zeitschrift für Physik*, 43, 172–198.
- Hopkinson, C., Chasmer, L., Lim, K., Treitz, P., & Creed, I. (2006). Towards a universal lidar canopy height indicator. *Canadian Journal of Remote Sensing*, 32(2), 139–153.
- Hopkinson, C., Chasmer, L., Colville, D., Fournier, R., Hall, R., Luther, J., ... St-Onge, B. (2013). Moving towards consistent ALS monitoring of forest attributes across Canada; the 'C-CLEAR' approach. *Photogrammetric Engineering and Remote Sensing*, 79(2), 159–173.
- Hopkinson, C., Chasmer, L., & Hall, R. (2008). The uncertainty in conifer plantation growth prediction from multi-temporal lidar datasets. *Remote Sensing of Environment*, 112(3), 1168–1180.
- Howard, E. A., Gower, S. T., Foley, J., & Kucharik, C. J. (2004). Effects of logging on carbon dynamics of a jack pine forest in Saskatchewan, Canada. *Global Change Biology*, 10, 1267–1284.
- Hudak, A. T., Strand, E. K., Vierling, L. A., Byrne, J. C., Eitel, J. U. H., Martinuzzi, S., & Falkowski, M. J. (2012). Quantifying aboveground forest carbon pools and fluxes from repeat LiDAR surveys. *Remote Sensing of Environment*, 123, 25–40.
- IPCC (2013). Climate change 2013: The physical science basis. Contribution of Working Group I to the Fifth assessment report of the Intergovernmental Panel on Climate Change [Stocker, T.F., D. Qin, G.-K. Plattner, M. Tignor, S.K. Allen, J. Boschung, A. Nauels, Y. Xia, V. Bex and P.M. Midgley (eds.)]. Cambridge University Press, Cambridge, United Kingdom and New York, NY, USA, doi:<http://dx.doi.org/10.1017/CBO9781107415324>, (1535 pp.)
- Jandl, R., Lindner, M., Vesterdal, L., Bauwens, B., Baritz, R., Hagedorn, F., ... Byrne, K. A. (2007). How strongly can forest management influence soil carbon sequestration? *Geoderma*, 137(3–4), 253–268.
- Jung, M., Reichstein, M., Margolis, H. A., Cescatti, A., Richardson, A. D., Arain, M. A., ... Williams, C. (2011). Global patterns of land-atmosphere fluxes of carbon dioxide, latent heat, and sensible heat derived from eddy covariance, satellite and meteorological observations. *Journal of Geophysical Research*, 116, G00J07. <http://dx.doi.org/10.1029/2010JG001566>.
- Kljun, N., Black, T. A., Griffis, T. J., Barr, A. G., Gaumont-Guay, D., Morgenstern, K., ... Nestic, Z. (2007). Response of net ecosystem productivity of three boreal forest stands to drought. *Ecosystems*, 10, 1039–1055.
- Kljun, N., Calanca, P., Rotach, M. W., & Schmid, H. P. (2004). A simple parameterisation for flux footprint predictions. *Boundary-Layer Meteorology*, 112, 503–523.
- Kljun, N., Rotach, M. W., & Schmid, H. P. (2002). A 3D backward Lagrangian footprint model for a wide range of boundary layer stratifications. *Boundary-Layer Meteorology*, 103, 205–226.
- Kristensen, T., Næsset, E., Ohlson, M., Bolstad, P. V., & Kolka, R. (2015). Mapping above- and below-ground carbon pools in boreal forests: The case for airborne lidar. *PLoS One*. <http://dx.doi.org/10.1371/journal.pone.0128450> (24 pp.).
- Kurz, W. A., & Apps, M. J. (1999). A 70-year retrospective analysis of carbon fluxes in the Canadian Forest Sector. *Ecological Applications*, 9(2), 526–547.
- Kurz, W., Shaw, C. H., Boisvenue, C., Stinson, G., Metsaranta, J., Leckie, D., ... Neilson, E. T. (2013). Carbon in Canada's boreal forest – A synthesis. *Environmental Review*, 21, 260–292.
- Lal, R. (2005). Forest soils and carbon sequestration. *Forest Ecology and Management*, 220, 242–258.
- Lambert, M. -C., Ung, C. -H., & Raulier, F. (2005). Canadian national tree aboveground biomass equations. *Canadian Journal of Forest Research*, 35, 1996–2018.
- Law, B. E., Thornton, P. E., Irvine, J., Anthoni, P. M., & Van Tuyl, S. (2001). Carbon storage and fluxes in ponderosa pine forests at different developmental stages. *Global Change Biology*, 7(7), 755–777.
- Leclerc, M. Y., & Foken, T. (2014). *Footprints in micrometeorology and ecology* (1st ed.). Heidelberg, Germany, New York, USA, Dordrecht, the Netherlands, London, UK: Springer.
- Lehtonen, A., Makipaa, R., Heikkinen, J., Sievanen, R., & Liski, J. (2004). Biomass expansion factors (BEFs) for Scots pine, Norway spruce and birch according to stand age for boreal forests. *Forest Ecology and Management*, 188, 211–224.
- Little, E. L., Jr. (1971). Atlas of United States trees. *Conifers and important hardwoods*. Miscellaneous publication 1146, Vol. 1, Washington, DC: U.S. Department of Agriculture, Forest Service (9 pp.).
- Litton, C. M., Raich, J. W., & Ryan, M. G. (2007). Carbon allocation in forest ecosystems. *Global Change Biology*, 13, 2089–2109. <http://dx.doi.org/10.1111/j.1365-2486.2007.01420.x>.
- Litton, C. M., Ryan, M. G., & Knight, D. H. (2004). Effects of tree density and stand age on carbon allocation patterns in postfire lodgepole pine. *Ecological Applications*, 14(2), 460–475.
- Lovett, G. M., Cole, J. J., & Pace, M. L. (2006). Is ecosystem production equal to ecosystem carbon accumulation? *Ecosystems*, 9, 152–155.
- Means, J. E., Acker, S. A., Harding, D. J., Blair, J. B., Lefsky, M. A., Cohen, W. B., ... McKee, W. A. (1999). Use of large-footprint scanning airborne lidar to estimate forest stand characteristics in the Western Cascades of Oregon. *Remote Sensing of Environment*, 67, 298–308.
- Medvigy, D., & Moorcroft, P. R. (2011). Predicting ecosystem dynamics at regional scales: An evaluation of a terrestrial biosphere model for the forests of northeastern North America. *Philosophical Transactions of the Royal Society B*, 367, 222–235.
- Montwé, D., Spiecker, H., & Hamann, A. (2014). An experimentally controlled extreme drought in a Norway spruce forest reveals fast hydraulic response and subsequent recovery of growth rates. *Trees*, 28, 891–900. <http://dx.doi.org/10.1007/s00468-014-1002-5>.
- Næsset, E., & Gobakken, T. (2005). Estimating forest growth using canopy metrics derived from airborne laser scanner data. *Remote Sensing of Environment*, 96(3–4), 453–465.
- Næsset, E., & Gobakken, T. (2008). Estimation of above- and below-ground biomass across regions of the boreal zone using airborne laser. *Remote Sensing of Environment*, 112(6), 3079–3090.
- Næsset, E., Bollandsås, O. M., Gobakken, T., Gregoire, T., & Ståhl, G. (2013). Model-assisted estimation of change in forest biomass over an 11 year period in a sample survey supported by airborne LiDAR: A case study with post-stratification to provide "activity data". *Remote Sensing of Environment*, 128, 299–314.
- Økseter, R., Bollandsås, O. M., Gobakken, T., & Næsset, E. (2015). Modeling and predicting aboveground biomass change in young forest using multi-temporal airborne laser scanner data. *Scandinavian Journal of Forest Research*, 30(5), 458–469.
- Peichl, M., & Arain, M. A. (2007). Allometry and partitioning of above- and belowground tree biomass in an age-sequence of white pine forests. *Forest Ecology and Management*, 253, 68–80.
- Peichl, M., Brodeur, J. J., Khomik, M., & Arain, M. A. (2010). Biometric and eddy-covariance based estimates of carbon fluxes in an age-sequence of temperate pine forests. *Agricultural and Forest Meteorology*, 150, 952–965.
- Popescu, S. C., Wynne, R. H., & Nelson, R. F. (2003). Measuring individual tree crown diameter with lidar and assessing its influence on estimating forest volume and biomass. *Canadian Journal of Remote Sensing*, 29(5), 564–577.
- Pregitzer, K. S., & Euskirchen, E. (2004). Carbon cycling and storage in world forests: Biome patterns related to forest age. *Global Change Biology*, 10(12), 2052–2077. <http://dx.doi.org/10.1111/j.1365-2486.2004.00866.x>.

- Randerson, T. J., Chapin, F. S., III, Harden, J. W., Neff, J. C., & Harmon, M. E. (2002). Net ecosystem production: A comprehensive measure of net carbon accumulation by ecosystems. *Ecological Applications*, 12(4), 937–947.
- Ryan, M. G., Binkley, D., Fownes, J. H., Giardina, C. P., & Senock, R. S. (2004). An experimental test of the causes of forest growth decline with stand age. *Ecological Monographs*, 74(3), 393–414.
- Schmid, H. P. (1994). Source areas for scalars and scalar fluxes. *Boundary-Layer Meteorology*, 67(3), 293–318.
- Sellers, P., Hall, F., Ranson, K. J., Margolis, H., Kelly, B., Baldocchi, D., ... Wickland, D. E. (1995). The Boreal Ecosystem–Atmosphere Study (BOREAS): An overview and early results from the 1994 field year. *Bulletin of the American Meteorological Society*, 76, 1549–1577.
- Semboli, O., Beina, D., Closset-Kopp, D., Gourlet-Fleury, S., & Decocq, G. (2014). Does long-term monitoring of tropical forests using permanent plots provide unbiased results? *Applied Vegetation Science*. <http://dx.doi.org/10.1111/avsc.12097>.
- Skowronski, N. S., Clark, K. L., Gallagher, M., Birdsey, R. A., & Hom, J. L. (2014). Airborne laser scanner-assisted estimation of aboveground biomass change in a temperate oak-pine forest. *Remote Sensing of Environment*, 151, 166–174.
- Stoker, J. M., Cochrane, M. A., & Roy, D. P. (2013). Integrating disparate lidar data at the national scale to assess the relationships between height above ground, land cover and ecoregions. *Photogrammetric Engineering and Remote Sensing*, 80(1), 59–70.
- Theede, A. (2007). *Biometric and eddy-covariance estimates of ecosystem carbon storage at two boreal forest stands in Saskatchewan: 1994–2004*. (Master's Thesis submitted to the University of Saskatchewan, Saskatoon Sask. Canada. 129 pp.).
- Tobin, B., & Nieuwenhuis, M. (2007). Biomass expansion factors for Sitka spruce (*Picea sitchensis* (Bong.) Carr.) in Ireland. *European Journal of Forest Research*, 126, 189–196.
- Van Tuyl, S., Law, B. E., Turner, D. P., & Gitelman, A. I. (2005). Variability in net primary production and carbon storage in biomass across Oregon forests – An assessment integrating data from forest inventories, intensive sites, and remote sensing, 2005. *Forest Ecology and Management*, 206, 273–291.
- Vesala, T., Kljun, N., Rannik, U., Rinne, J., Sogachev, A., Markkanen, T., ... Leclerc, M. (2008). Flux and concentration footprint modelling: State of the art. *Environmental Pollution*, 152(3), 653–666.
- Vogel, J. G., & Gower, S. T. (1998). Carbon and nitrogen dynamics of boreal jack pine stands with and without a green alder understory. *Ecosystems*, 1, 386–400.
- Wulder, M. A., White, J. C., Bater, C. W., Coops, N. C., Hopkins, C., & Chen, G. (2012). Lidar plots – A new large-area data collection option: Context, concepts, and case study. *Canadian Journal of Remote Sensing*, 38(5), 600–618.
- Zha, T. S., Barr, A. G., Bernier, P. -Y., Lavigne, M. B., Trofymow, J. A., Amiro, B. D., ... Coursolle, C. (2013). Gross and aboveground net primary production at Canadian forest carbon flux sites. *Agricultural and Forest Meteorology*, 174–175, 54–64.
- Zhao, M., Heinsch, F. A., Nemani, R. R., & Running, S. W. (2005). Improvements of the MODIS terrestrial gross and net primary production global data set. *Remote Sensing of Environment*, 95(2), 164–176.